RADAR CLUTER CLASSIFICATION USING AUTOREGRESSIVE MODELLING, K-DISTRIBUTION AND NEURAL NETWORK

C. Bouvier*, L. Martinet*, G. Favier**, H. Sedano* and M. Artaud*

* DCN - STSN/CTSN - Centre Technique des systèmes navals - Lutte Surface Air - Service Traitement du signal et de l'information, B.P. 28, 83800 TOULON NAVAL FRANCE

** I3S Laboratory, CNRS/UNSA, Bât. SPI n°4, 250 rue Albert Einstein, Sophia Antipolis, F-06560 VALBONNE

ABSTRACT

This paper is concerned with the classification of radar returns including sea, ground and composite clutters. We first present an analysis of radar clutter recorded data allowing to validate the K amplitude distribution and the autoregressive modelling of the spectrum.

Then, we briefly describe a classifier based on a multi-layer neural network. The inputs of which are the shape parameter of the K-distribution, the magnitude and the phase of the poles and the reflection coefficients calculated by means of the Burg's or multi-segment algorithm. Experimental results are presented to illustrate the performance of the proposed classifier

1 INTRODUCTION

Separation of moving targets and clutter signals due to sea and ground and also due to birds, storm clouds or other atmospheric dirsturbances, is an important step in radar signal processing. This separation allows us not only to considerably improve radar detection performances, but also to identify clutter in order to make decisions for the control of air traffic or for the control of the radar itself. It is therefore important to classify radar clutter signals, which is the subject of this paper.

Clutter models have to fulfil certain constraints in both amplitude distribution and correlation properties, i.e. spectral characteristics. As a consequence of the central limit theorem, the sea clutter amplitude distribution is often assumed to be the Rayleigh distribution. However, for low grazing angles and/or high-resolution radars, the empirical distributions calculated from experimental data exhibit significant deviations from Rayleigh statistics. This is why the K-distribution has received the most attention. Moreover, the K-distribution has been validated by experimental data [1, 2, 3], and unlike the Weibull distribution, has physical interpretations [4]. The compound form of the K-distribution allows us to identify two components of clutter fluctuations. The first, corresponding to an instantaneous component, accounts for the reflection from a very large number of independent, identically distributed elementary scatterers; it varies rapidly and exhibits a decorrelation time of a few milliseconds, depending on the internal motion of the scatterers within each resolution cell as well as on the radar wavelength. The second component, corresponding to a mean component, is a spatially vary$ing mean level resulting from a bunching of scatterers associated with the sea swell structure. This component varies slowly with a long correlation time of several seconds, and is unaffected by frequency agility. The properties of this component are studied in [5]. Based on both experimental analysis and theorical reasoning, it is shown in [6] that ground clutter also obeys the K-distribution.

Concerning the correlation properties of the clutter, its power spectrum can be modeled by using high resolution spectral methods, which give the clutter model as a combination of spectral lines for sea clutter [7] or by means of a low order autoregressive model for both sea and ground clutter [8, 9, 10].

For classification purposes, it is shown in [8] that spectral characteristics in terms of reflection coefficients, autoregressive parameters and cepstral coefficients, could be used as discriminant features for classifying radar ground clutter by means of a traditional Bayes classifier. In [11], classification of several types of radar returns including birds, weather and aircraft was carried out using both reflection coefficients obtained from a second-order spectral analysis, higher order statistics (skewness and kurtosis which measure the degree of deviation of the incoming radar data from Gaussianity), and signal-strength-related features.

In this paper, we present firstly an analysis of recorded radar clutter data allowing us to validate the K amplitude distribution and the autoregressive modelling of the spectrum. In the second part, we propose a neural network based classifier to distinguish between sea, ground and composite clutters. Some experimental results are described to illustrate the behavior of this classifier.

2 FEATURE SELECTION

2.1 Experimental data

Clutter data were recorded from an S-band radar functioning in operation mode on the Mediterranean seashore. This radar is a

0-7803-2431-5/95 $4.00 © 1995 IEEE

two dimension (azimuth and range) surveillance radar. It is able to operate with the agility of the emission frequency and wobbulation of the pulse repetition frequency, so the data coherence time is short and corresponds to a duration of one single burst of less than ten pulses.

The observations of sea clutter were recorded for several directions of propagation of the swell and for different meteorological conditions, from a calm sea (sea state 2) to a rough sea (sea state 4). Land clutter have been recorded both on flat and on cliff seashores.

Four classes of echos were distingished in these data: land clutter, calm sea clutter, rough sea clutter and a composite clutter class in which most of the energy comes from atmospheric clutter or thermal noise.

2.2 Amplitude distribution characteristics

First, we tested the goodness-of-fit of the Weibull, Rayleigh and K distributions on real data. The results showed the good fit of the K-distribution whatever the experimental conditions. The K-distribution is depicted by (1).

$$P(x)=\frac{2b}{\Gamma(\nu)}\left(\frac{bx}{2}\right)^{\nu}\mathrm{K}_{\nu-1}(bx) \quad x\geq 0 \qquad (1)$$

The two parameters of the K-distributions, b and ν, are correlated. Indeed, the ratio $4\nu/b^2$ is related to the energy and thus dependent on range. The shape parameter ν takes alone, represents the texture of the clutter. Homogeneous clutters lead to high values for ν, while strong returns such as land clutter are represented with small values. Fig. 1 shows K-distributions for four different types of clutter: calm sea, rough sea, land and composite clutter.

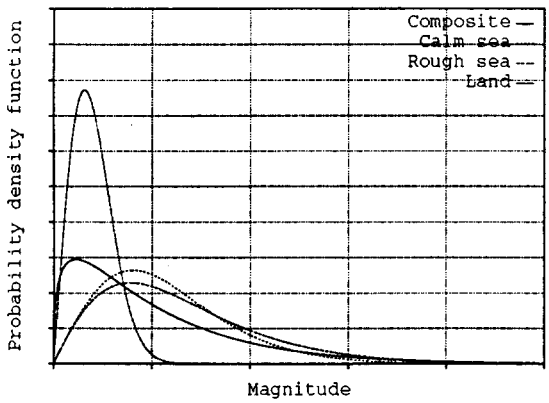

Fig. 1 : *K-distributions for 4 different types of clutter.*

The values of the shape parameters ν are given in Tab. 1 for four different types of clutter . This shape parameter proves to be useful as a feature for clutter classification.

Land clutter	*Rough sea clutter*	*Calm sea clutter*	*Composite clutter*
0.7	2.4	5.1	29

Tab. 1 : *K-distribution shape parameter for four different types of clutter.*

2.3 Spectral characteristics

The results of spectral analysis performed on short time data (duration of one single burst), show that autoregressive modelling is well adapted to represent the sea clutter spectrum. A second order model was sufficient to obtain a good representation. Our statistical analysis of the first AR pole shows that the magnitude and phase have different values according to the type of clutter. Fig. 2 and 3 respectively, plot the first AR pole computed with the Burg's algorithm for land and rough sea clutters.

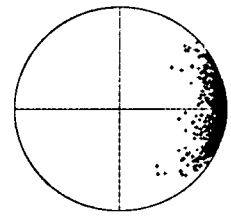

Fig. 2 : *Rough sea* .

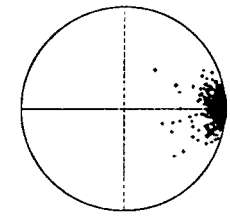

Fig. 3 : *Land.*

A better discrimination can be obtained with the multi-segment algorithm [11] for computing the reflection coefficients, which gives results averaged in space (range gates and burst) and time (antenna scans). The M order reflection coefficients are then calculated by means of (2).

$$\rho_M=\frac{-2\sum_{s=1}^{S}\sum_{g=1}^{G}\sum_{b=1}^{B}\sum_{n=M+1}^{N_B} f_{n,b,g,s}^{(M-1)}\,b_{n-1,b,g,s}^{(M-1)*}}{\sum_{s=1}^{S}\sum_{g=1}^{G}\sum_{b=1}^{B}\sum_{n=M+1}^{N_B}\left[\left|f_{n,b,g,s}^{(M-1)}\right|^2+\left|b_{n-1,b,g,s}^{(M-1)}\right|^2\right]} \qquad (2)$$

where M represents the AR filter order, S the number of scans, G the number of gates, B the number of bursts and N_B the number of samples in the burst b. Fig. 4 and 5 plot the first AR poles obtained with the multi-segment algorithm, in processing the same data as for Fig. 2 and 3.

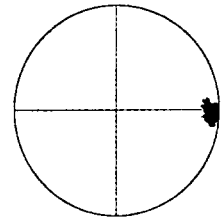

Fig. 4 : *Rough sea* .

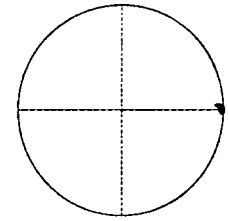

Fig. 5 : *Land.*

3 NEURAL NETWORK BASED CLASSIFIER

For radar clutter classification, we used a multi-layer neural network with one or two hidden layers. The learning algorithm is the back-propagation method. The output layer is composed of four neurons corresponding to the four classes of radar clutter described in § 2.1.
Theirs inputs are both amplitude characteristics with the shape parameter of the K-distribution and spectral characteristics with the reflection coefficients or the poles calculated with the Burg's algorithm or its multi-segment version. The input layer is then composed of five neurons.

4 EXPERIMENTAL RESULTS

The performances are measured in terms of classification rate for each class, and Average Classification Rate (ACR) in percent. Two different data sets composed of 9520 samples (a sample is the features calculated on the corresponding burst) for each class, were used as training examples and testing data for generalization.

We first determinated the best discriminant features among the spectral parameters (magnitude and phase of the poles or the relflection coefficients associated with a first or second order AR model) estimated in using the Burg's algorithm. Then, the influence of the neural network architecture (number of hidden layers and number of neurons in each hidden layer) was studied. Finally, performance improvements have been obtained by considering the multi-segment algorithm for computing the poles, and by incorporating the K-distribution shape parameter as a supplementary discriminant feature.

4.1 Determination of the best spectral parameters as discriminant features

The comparison of the classifier performances was carried out in terms of the ACR, with a 1-9-4 architecture, i.E. one neuron on the first layer (input corresponding to the spectral parameter), nine neurons on the hidden layer and four neurons on the output layer. The best performance (ACR of 44.04%) was obtained with the magnitude of the fisrt reflection coefficient. We can note that this feature is related to the spectral width of the process.
When using two discriminant features, the best ACR (47.38%) was obtained with the phase of the poles of a second order AR model. If the magnitude and the phase are used, i.e. with a 4-9-4 architecture, the best classification results (ACR of 57.48%) are also obtaines with the poles.
From this experimental study, it was decided to consider the magnitude and the phase of the poles of a second order AR model as discriminant features.

4.2 Determination of the network architecture, and comparison of estimation algorithms

Fig. 6 and Fig. 7 show the ACR for different network architectures, depending on the number (one or two) of hidden layers and the number of neurons (two to thirteen) in each hidden layer when the poles are calculated by means of the Burg's or the multi-segment (with S=3, G=5 and B=5) algorithms respectively.

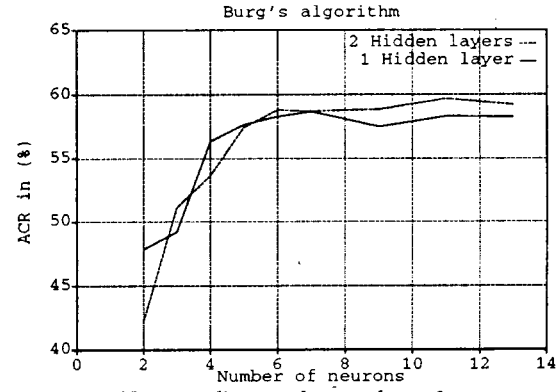

Fig. 6 : *ACR according to the number of neurons.*

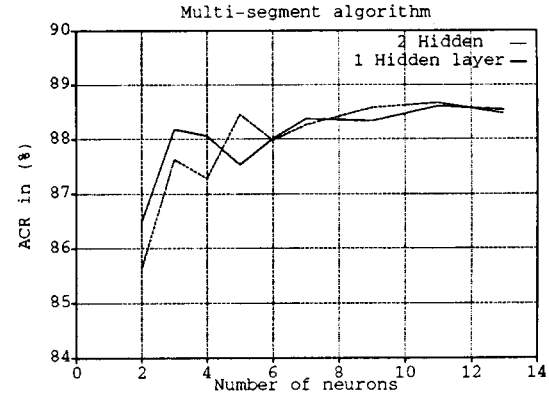

Fig. 7 : *ACR according to the number of neurons.*

The best classification results are obtained with a 4-11-11-4 architecture, i.e. two hidden layers with eleven neurons in each hidden layer. However, almost the same performances are obtained with nine neurons in the hidden layers, so that a 4-9-9-4 architecture provides a good compromise between classification performances and computation time.

Finally, in comparing Fig. 6 and 7, we conclude that the use of the multi-segment algorithm to estimate the poles improves significantly the classifier performances.
Indeed, the averaging in space, on both the range and azimuth, allows us to take into account the spatial correlation that is different according to the type of clutter, while the averaging in time (antenna scans) allows us to take into account the time

correlation which is important for land clutter (due to immobile reflectors, radar returns are highly correlated from scan to scan). A good compromise between computation time and classification performance was obtained with S=3, G=5 and B=5.

4.3 Classification results

The classification results obtained with a 4-9-9-4 network and with the poles calculated with the multi-segment algorithm (S=3, G=5 and B=5) are summarized in Tab. 2.
The results in generalization (ACR of 89.3%), close to the results obtained during the training step (88.6% and 88.2% for the training data 1 and 2 respectively) prove the good behavior of the classifier. We notice from the results, that land and composite clutters are recognized more accurately than sea clutter. The separation between a calm and a rough sea is a difficult task, due to the same nature of the two classes.

4.4 Use of the K-distribution shape parameter

In this section we introduce the shape parameter of the K-distribution as a discriminant feature. When this shape parameter is used alone, the ACR is about 71.7%. By considering both the poles and the shape parameter as inputs of the neural network (i.e. with a 5-9-9-4 architecture), we get an ACR of 96.5% during the training step. But, in the generalization step the ACR decreases to 70%. This is due to the non stationarity of the shape parameter estimation between the training and testing steps.

5 CONCLUSION

In this paper, we have proposed a multi-layer neural network based classifier for distinguishing several recorded radar returns in a real operational mode: land, sea and composite clutters. By using spectral parameters as the inputs of the neural network, an ACR of 89.3% was obtained during the generalization step. Such a solution could be used for radar clutter segmentation during an operational mode.
We have shown that the classifier performances can be improved in taking the K-distribution shape parameter into account. However, due to the non stationarity of the shape parameter estimation, its incorporation as an input of the neural network needs further studies effective concerning the generalization step.

	Classification results				
Data	Land (%)	Calm sea (%)	Rough sea (%)	Composite (%)	ACR (%)
Training data 1	99.4	69.4	85.6	100	88.6
Training data 2	98.6	71.7	82.7	99.9	88.2
Testing data	98.6	76.4	82.2	100	89.3

Tab 2. : *Summary of classification results on testing and training data.*

REFERENCES

[1] C. J. BAKER
K-distributed coherent sea clutter, IEE Proceedings-F, Vol. 138, N°2, PP. 89-92, April 1991.

[2] C. J. OLIVER
Representation of radar sea clutter, IEE Proceedings, Vol. 135, Pt. F, N°6, PP. 497-500, December 1988.

[3] K. D. WARD
A radar clutter model and its application to performance assessment, IEE EW series 20, PP. 217-221, 1985.

[4] E. JAKEMAN and P. N. PUSEY
Statistics of non-Rayleigh microwave sea echo , IEEE Int. Radar Conf., PP. 105-109, 1977.

[5] C. J. OLIVER
Correlated K-distributed clutter models, Optica Acta, Vol. 32, N°12, PP. 1515-1547, 1985.

[6] J. K. JAO
Amplitude distribution of composite terrain radar clutter and the K-distribution, IEEE Trans Antennas and propagation, Vol. 32, N°10, PP. 1049-1062, October 1984.

[7] J. P. HENRY
Amplitude and spectral characterization of radar sea clutter, International Radar Conference, Paris , PP. 126-131, 1989.

[8] J.-F. AGNEL
Modélisation et classification de fouillis de sols. Application à la reconnaissance, International Radar Conference, Paris , session AIII, PP. 109-114, 1984.

[9] S. HAYKIN, W. STEHWIEN, C. DENG, P. WEBER and R. MANN
Classification of radar clutter in air traffic control environment, Proceedings of the IEEE, Vol. 79, N°6, PP. 742-772, June 1991.

[10] S. HAYKIN, B. W. CURRIE and S. B. KESLER
Maximum-Entropy Spectral Analysis of Radar Clutter, Proceedings of the IEEE, Vol. 70, N°9, PP. 953-962, September 1982.

[11] S. HAYKIN and C. DENG
Classification of radar clutter using neural networks, IEEE Transactions on Neural Networks, Vol. 2, N°6, PP. 589-600, 1991.